General Disclaimer

One or more of the Following Statements may affect this Document

- This document has been reproduced from the best copy furnished by the organizational source. It is being released in the interest of making available as much information as possible.

- This document may contain data, which exceeds the sheet parameters. It was furnished in this condition by the organizational source and is the best copy available.

- This document may contain tone-on-tone or color graphs, charts and/or pictures, which have been reproduced in black and white.

- This document is paginated as submitted by the original source.

- Portions of this document are not fully legible due to the historical nature of some of the material. However, it is the best reproduction available from the original submission.

Produced by the NASA Center for Aerospace Information (CASI)

NASA Technical Memorandum 78677

SUBSONIC ROLL DAMPING OF A MODEL WITH SWEPT-BACK
AND SWEPT-FORWARD WINGS

RICHMOND P. BOYDEN

MARCH 1978

INTRODUCTION

Swept-back wings have been widely used on transonic and supersonic aircraft to delay the effects of transonic compressibility and thereby achieve satisfactory performance at high speeds. As is well known, swept-forward wings are also a possible solution to the transonic compressibility problem, but the structural design and weight of swept-forward wings has been plagued by the problem of bending-torsion divergence (see references 1 and 2). However, a recent paper (reference 3) on the use of advanced composite materials with optimized orientation and thickness shows promise as a means of alleviating the weight penalty previously associated with the use of swept-forward wings on high-speed aircraft.

The objective of this study was to obtain some comparative aerodynamic roll damping data at subsonic speeds on swept-back and swept-forward wings on a general research fighter configuration fuselage. The forced-oscillation roll technique was used to determine the roll damping and the yawing moment due to roll rate. This investigation was conducted in the Langley high-speed 7- by 10-foot tunnel at Mach numbers ranging from 0.3 to 0.7 and angles of attack from $-4°$ to about $20°$. It should be noted that the model wing panels used in this study were designed and constructed for tests of swept-back wing configurations having sharp leading edges. The fact that the wing panels have circular arc sections made it feasible to utilize these existing wing panels in

the reversed or swept-forward orientation. It must be kept in mind
however, that because of the flow separation at the sharp leading edges
that this data should not be expected to be indicative of the damping
characteristics of thick, rounded leading-edge wings.

The static longitudinal and lateral-directional aerodynamic
characteristics of swept-back and swept-forward wing configurations
utilizing the same wing panels as the present study are included in
reference 4.

Some previous tests of the roll damping of isolated swept-forward
wings at low speeds are reported on in references 5 to 7.

SYMBOLS

The aerodynamic parameters in this report are referred to the body system of axes as shown in figure 1 in which the coefficients, angles and angular velocity are shown in the positive sense. These axes originate at the moment reference center which was located according to the model drawings in figure 2.

Units of measurement are presented in the International System of Units (SI). Details on the use of SI together with the physical constants and conversion factors are given in reference 8.

b	reference span, 0.5436 meter
$\bar{c}$	mean geometric chord, 0.2456 meter
f	frequency of oscillation, hertz
k	reduced-frequency parameter, $\omega b/2V$, radians
M	free-stream Mach number
p	angular velocity of model about X-axis, radians/second
q_∞	free-stream dynamic pressure, pascals
R	Reynolds number based on $\bar{c}$
S	reference area, 0.1156 meter^2
V	free-stream velocity, meters/second

X,Y,Z   reference body axes

α   angle of attack, degrees

β   angle of sideslip, degrees

ω   angular velocity, $2\pi f$, radians/second

C_l rolling-moment coefficient, Rolling moment/$q_\infty Sb$

C_n yawing-moment coefficient, Yawing moment/$q_\infty Sb$

$$C_{l_\beta} = \frac{\partial C_l}{\partial \beta} \quad \text{per radian}$$

$$C_{l_{\dot\beta}} = \frac{\partial C_l}{\partial \left(\frac{\dot\beta b}{2V}\right)} \quad \text{per radian}$$

$$C_{l_p} = \frac{\partial C_l}{\partial \left(\frac{pb}{2V}\right)} \quad \text{per radian}$$

$$C_{l_{\dot p}} = \frac{\partial C_l}{\partial \left(\frac{\dot p b^2}{4V^2}\right)} \quad \text{per radian}$$

$C_{l_\beta} \sin \alpha - k^2 C_{l_{\dot{p}}}$ rolling moment due to roll displacement parameter, per radian

$C_{l_p} + C_{l_{\dot{\beta}}} \sin \alpha$ damping-in-roll parameter, per radian

$$C_{n_\beta} = \frac{\partial C_n}{\partial \beta} \text{ per radian}$$

$$C_{n_{\dot{\beta}}} = \frac{\partial C_n}{\partial \left(\frac{\dot{\beta}b}{2V}\right)} \text{ per radian}$$

$$C_{n_p} = \frac{\partial C_n}{\partial \left(\frac{pb}{2V}\right)} \text{ per radian}$$

$$C_{n_{\dot{p}}} = \frac{\partial C_n}{\partial \left(\frac{\dot{p}b^2}{4V^2}\right)} \text{ per radian}$$

$C_{n_\beta} \sin \alpha - k^2 C_{n_{\dot{p}}}$ yawing moment due to roll displacement parameter, per radian

$C_{n_p} + C_{n_{\dot{\beta}}} \sin \alpha$ yawing moment due to roll rate parameter, per radian

A dot over a quantity indicates a first derivative with respect to time.

Model component designations:

B	body
V	vertical tail
W	wing
H	horizontal tail

MODEL AND TEST APPARATUS

Three-view drawings of the model with the wing in both the swept-back and in the swept-forward configuration are shown in figure 2. The same uncambered and untwisted wing panels with circular arc airfoil sections were used for all configurations. The wing had a nominal leading-edge sweep of 60° in the swept-back configuration and a nominal -32° leading edge sweep in the swept-forward configuration. By reversing the wing, the half-chord sweep remains the same magnitude implying approximately the same structural span. The horizontal and vertical tail surfaces had a leading-edge sweep of 51.7° and each of the three panels had the same dimensions. Detailed geometric characteristics of the model are listed in Table I.

A photograph of the model with the wings in the swept-forward orientation mounted on the sting for the forced-oscillation roll tests in the Langley high speed 7- by 10-foot tunnel is shown in figure 3. A description and the operating characteristics of the 7- by 10-foot wind tunnel can be found in reference 9. A photograph of the small-amplitude forced-oscillation roll balance is shown in figure 4. Reference 10 contains a detailed description of the oscillatory roll balance and the associated data-reduction procedure.

Tests

The dynamic stability parameters for the configuration with the wing in the 60° sweep-back orientation were measured at Mach numbers

of 0.4 and 0.7 while for the 32° swept-forward wing the tests were made at 0.3 and 0.7 Mach number. The nominal values of the wind tunnel test conditions are listed in Table II. The range of angle of attack available with the dynamic stability sting was from about -4° to 20°. The amplitude of the roll oscillation for this investigation was about 2.5° and was determined by the mechanical throw of the actuating crank. All of the data were taken with the models oscillating at the frequency for velocity resonance (see reference 10) which varied from about 6.42 to 8.31 hertz.

To insure a turbulent boundary layer over the model, carborundum grains were applied as three-dimensional roughness to the model nose and along the leading edge of the wing and the tail surfaces. The grit size and location were chosen based on the work in reference 11. The transition strips consisted of No. 120 carborundum grit applied in bands 0.16 cm wide located 2.54 cm aft of the model nose and 1.27 cm streamwise aft of the leading edge of the wing and the tail surfaces.

Results and Discussion

The effect of Mach number on the damping in roll parameter for the 60° swept-back wing configuration is shown in figure 5(a). The swept-back configuration had positive damping in roll over the angle of attack range and the roll damping did not fall below the 0° angle of attack value at any of the test conditions. The major difference between the results for the two Mach numbers was a peak in the roll damping at an

8

angle of attack of 12° for the 0.7 Mach number data. The rolling moment due to roll displacement parameter is included with the damping in roll parameter in the figures for completeness since the two components of rolling moment are measured at the same time. The usefulness of the rolling moment due to roll displacement parameter is reduced, however, because of the sin α multiplier in the C_{l_β} term. The parameter does serve to indicate the trends and sign changes of the dihederal effect. The 60° swept-back wing configuration in figure 5(a) is seen to have positive dihederal effect.

The yawing moment due to roll rate parameter for the 60° sweep configuration in the upper portion of figure 5(b) shows little variation with Mach number or angle of attack. The yawing moment due to roll displacement parameter in the lower part of figure 5(b) indicates there is positive directional stability over the range of angle of attack.

The damping in roll parameter for the swept-forward wing configuration is plotted in figure 6(a) for Mach numbers of 0.3 and 0.7. There is an increase in the roll damping up to an angle of attack of 8° to 10° and then a decrease with negative roll damping (positive values of the damping in roll parameter) at the highest angles of attack for both Mach numbers. This decrease in roll damping is presumed to be a result of tip stall or separation.

The 0.3 Mach number results for the swept-forward wing are compared with the 0.4 Mach number swept-back wing results in figure 7. The difference in the trends of the damping in roll for the two wing

orientations at angles of attack above 16° is obvious as is the difference in the levels of the rolling moment due to roll displacement parameter.

Figure 8 is a comparison of the swept-forward and swept-back wing configurations at a Mach number of 0.7. The decrease in roll damping of the swept-forward wing at the higher angles of attack compared to the swept-back wing is probably a result of the lower sweep angle of the wing in the swept-forward orientation. The probable vortex lift associated with the higher sweep of the swept-back wing might be expected to help maintain the damping while a more conventional stall might be expected for the low leading edge sweep of the forward-swept wing.

The effect of adding a horizontal tail to the swept-forward wing configuration is shown in figure 9 for a Mach number of 0.3. As would be expected there was a small increase in the roll damping as a result of the addition of the horizontal tail to the configuration.

In order to illustrate the type of differences that might be expected for round versus sharp leading-edge wings, the wing alone results of reference 6 are shown in figure 10 along with the present results. To provide a valid comparison with the present results, the data of reference 6 have been converted to the body axis system with the aid of the yawing data on the same wings from reference 12. The roll damping results from reference 6 do not include the $\dot{\beta}$ derivatives as those results were measured in the old Langley stability tunnel by holding the model fixed and forcing the air to flow around the model along a curved path. The wing models of reference 6 had NACA 0012 airfoil sections in planes normal to the leading edge and had untapered

planforms. The complete loss of damping at angles of attack above 19°
for the sharp-edged swept-forward wing configuration compared to the
60° swept-back wing configuration in figure 10(a) is attributed to the
combination of a sharp-edge wing and a relatively low leading-edge
sweep of -32°. However for the thick round leading edge wings of figure
10(b), the swept-back wing is seen to encounter a reduction in roll
damping at the higher angles of attack relative to the swept-forward
wing. This loss in roll damping for the swept-back wing with round leading
edges is thought to be a result of the increased local angle of attack
near the tip arising from the upwash from the forward portion of the
wing. The resulting higher tip loading for the swept-back wing would
result in tip stall occurring at a lower angle of attack compared to
the swept-forward wing of equal sweep where the inboard section of the
wing would carry the relatively higher loading. Since the thick round
leading edge wings would not be expected to develop vortex lift, a
reduction in roll damping results.

Concluding Remarks

An experimental investigation has been made into the roll damping
characteristics at subsonic speeds of a generalized fighter configuration
model with a swept-back or a swept-forward wing. Both wings had thin,
sharp leading edge airfoils. The configuration with a 60° swept-back
wing had positive damping in roll up to the maximum test angle of attack

11

of almost 20°. The 32° swept-forward wing configuration had positive roll damping at the lower angles of attack but there was a decrease in roll damping with increased angle of attack and negative roll damping was encountered at the highest angles of attack.

SUMMARY

The aerodynamic roll damping and the yawing moment due to roll rate characteristics were investigated at subsonic speeds for a model with either swept-back or swept-forward wings. The tests were made in the Langley high-speed 7- by 10-foot tunnel for Mach numbers between 0.3 and 0.7. The configuration with a 60° swept-back wing had positive damping in roll up to the maximum test angle of attack of almost 20°. The 32° swept-forward wing configuration had positive damping in roll at the lower angles of attack but there was a decrease in damping and negative damping in roll was measured at the highest angles of attack.

REFERENCES

1. Diederich, Franklin W.; and Budiansky, Bernard: Divergence of
    Swept Wings. NACA TN 1680, 1948.

2. Bisplinghoff, Raymond L.; Ashley, Holt; and Halfman, Robert L.:
    Aeroelasticity. Addison-Wesley Publishing Company, Reading,
    Massachusetts, 1955.

3. Krone, Norris J., Jr.: Divergence Elimination with Advanced
    Composites. AIAA Paper No. 75-1009, Aircraft Systems and Tech-
    nology Meeting, Los Angeles, California, August 1975.

4. Huffman, Jarrett K.; and Fox, Charles H., Jr.: Subsonic Longitudinal
    and Lateral-Directional Static Aerodynamic Characteristics for a
    Model with Swept Back and Swept Forward Wings. NASA TM 74093, 1977.

5. Maggin, Bernard; and Bennett, Charles V.: Low-Speed Stability and
    Damping-in-Roll Characteristics of Some Highly Swept Wings.
    NACA TN 1286, 1947.

6. Feigenbaum, David; and Goodman, Alex: Preliminary Investigation
    at Low Speeds of Swept Wings in Rolling Flow. NACA RM L7E09, 1947.

7. Hunton, Lynn W.; and Dew, Joseph K.: Measurements of the Damping
    in Roll of Large-Scale Swept-Forward and Swept-Back Wings.
    NACA RM A7D11, 1947.

8. Mechtly, E.A.: The International System of Units-Physical Constants
    and Conversion Factors (Second Revision). NASA SP-7012, 1973.

9. Fox, Charles H., Jr.; and Huffman, Jarrett K.: Calibration and
    Test Capabilities of the Langley 7- by 10-foot High Speed Tunnel.
    NASA TM X-74027, 1977.

10. Freeman, Delma C., Jr.; Boyden, Richmond P.; and Davenport, Edwin
    E.: Supersonic Dynamic Stability Characteristics of a Space
    Shuttle Orbiter. NASA TN D-8043, 1975.

11. Braslow, Albert L.; Hicks, Raymond M.; and Harris, Roy V., Jr.:
    Use of Grit-Type Boundary-Layer-Transition Trips on Wind-Tunnel
    Models. NASA TN D-3579, 1966.

12. Goodman, Alex; and Feigenbaum, David: Preliminary Investigation
    at Low Speeds of Swept Wings in Yawing Flow. NACA RM L7I09, 1948.

TABLE I – GEOMETRIC CHARACTERISTICS OF MODEL

Body length, cm   101.05

Body width, maximum, cm   11.18

Actual leading-edge sweep of nominal 60° sweep wing, deg   59.45

Actual leading-edge sweep of nominal -32° sweep wing, deg   -32.13

Wings

    Aspect ratio 2.56

    Span, cm 54.36

    Mean geometric chord, cm 24.56

    Area, cm^2 . . . . 1156.

    Root chord at fuselage juncture, cm 29.80

    Tip chord, cm 6.77

    Airfoil section . . . . circular arc

    Maximum thickness, percent chord, at –

       Root at fuselage juncture 6

       Tip 4

Horizontal tail

    Aspect ratio 2.77

    Span, cm 38.06

    Leading-edge sweep, deg 51.70

    Mean geometric chord, cm 16.23

    Area, cm^2 . . . . 522.6

    Root chord at fuselage juncture, cm 17.92

    Tip chord, cm 3.59

    Airfoil section . . . . circular arc

    Maximum thickness, percent chord, at –

       Root at fuselage juncture 6

       Tip 4

Vertical Tail

Aspect ratio 1.39

Span, cm 19.03

Leading-edge sweep, deg 51.70

Mean geometric chord, cm 16.23

Area, cm^2 . . . .   261.3

Root chord at fuselage juncture, cm 17.92

Tip chord, cm 3.59

Airfoil section . . . . circular arc

Maximum thickness, percent chord, at –

    Root at fuselage juncture   6

    Tip   4

TABLE II - NOMINAL TEST CONDITIONS

Mach number, M	Dynamic pressure, q_∞, kPa	Velocity, V, m/sec	Stagnation temperature T, K	Reynolds number, R	Reduced frequency parameter, k, radians
0.3	5.93	103	298	1.56×10^6	0.1063 to 0.1142
0.4	10.29	139	309	1.97	.0826 to .0938
0.7	25.33	235	308	3.02	.0848 to .0596
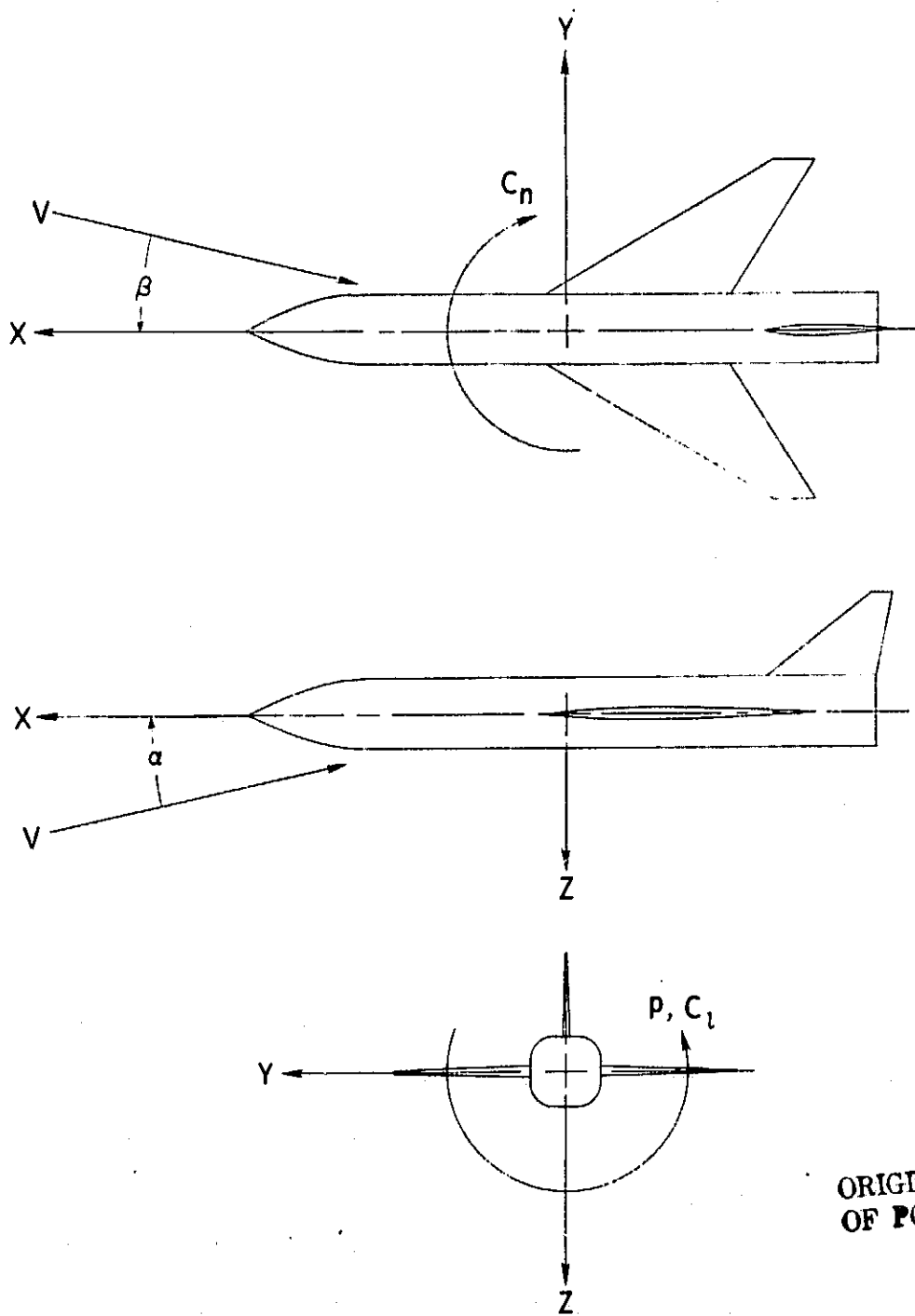
Figure 1. - Body system of axes with coefficients, angles, and angular velocity shown in the positive sense.

Moment reference center

54.36

11.18

47.65

59.45°

83.13

51.47

51.70°

13.44

11.18

101.05
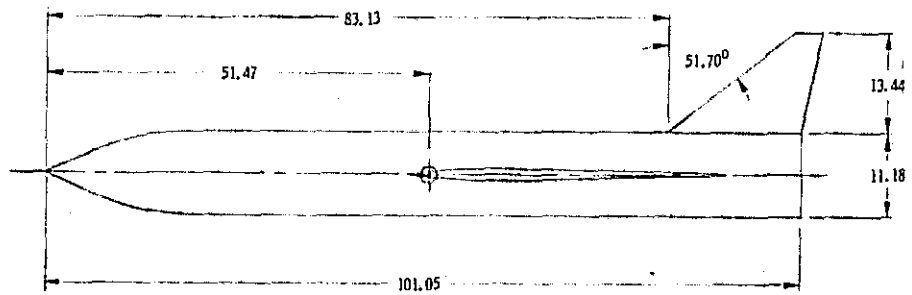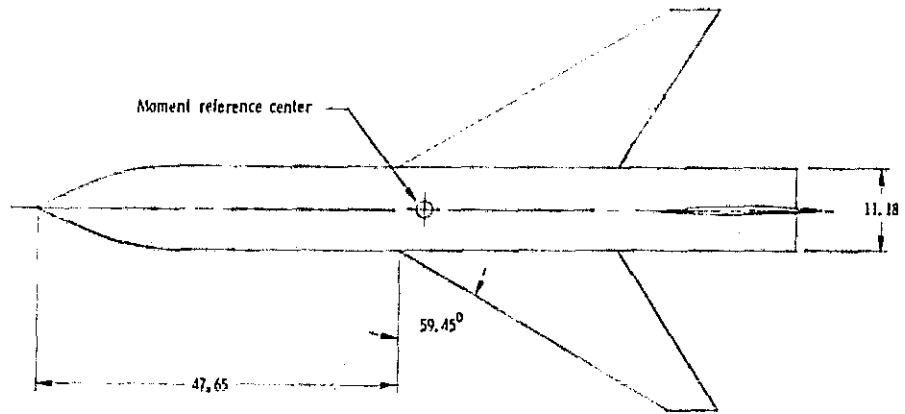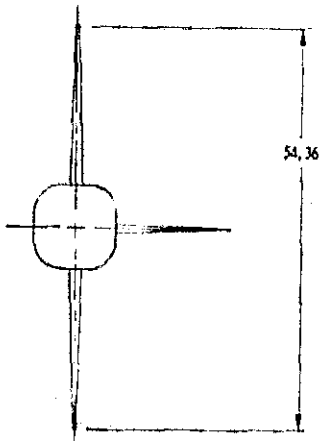
(a) 60° swept-back wing configuration

Figure 2.- General arrangement of models. All linear dimensions
are in centimeters.

83.13

54.36

Moment reference center

51.70°

38.06

11.18

32.13°

49.52

83.13

51.47

51.70°

13.44

11.18

4.29

101.05
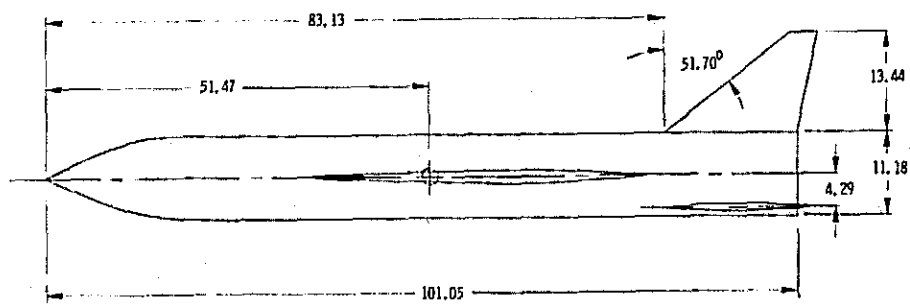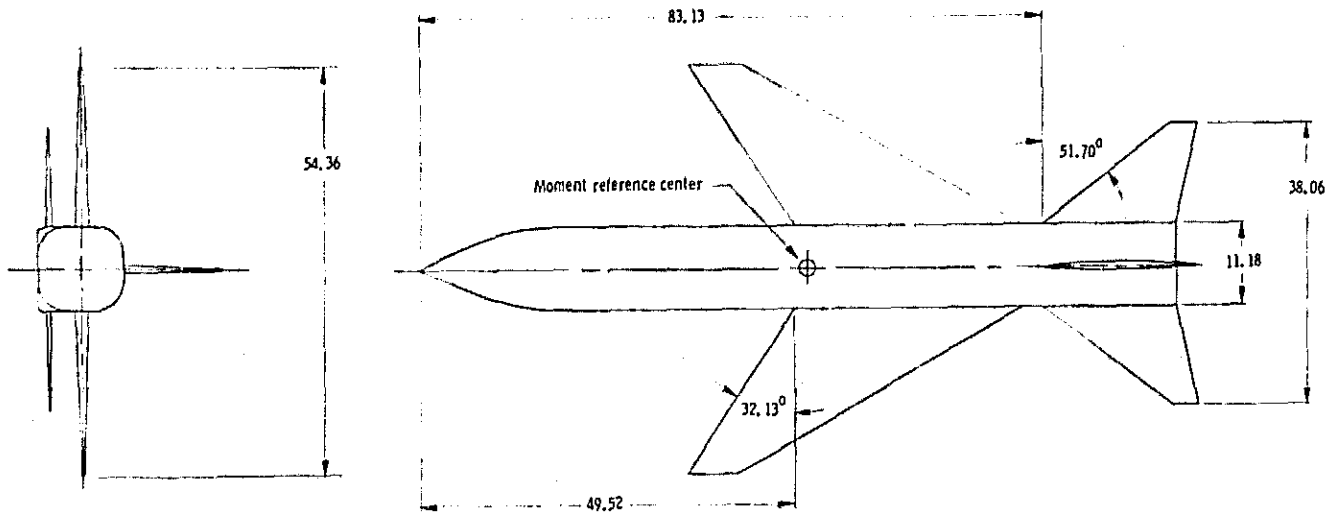
(b) 32° swept-forward wing configuration

Figure 2.- Concluded.
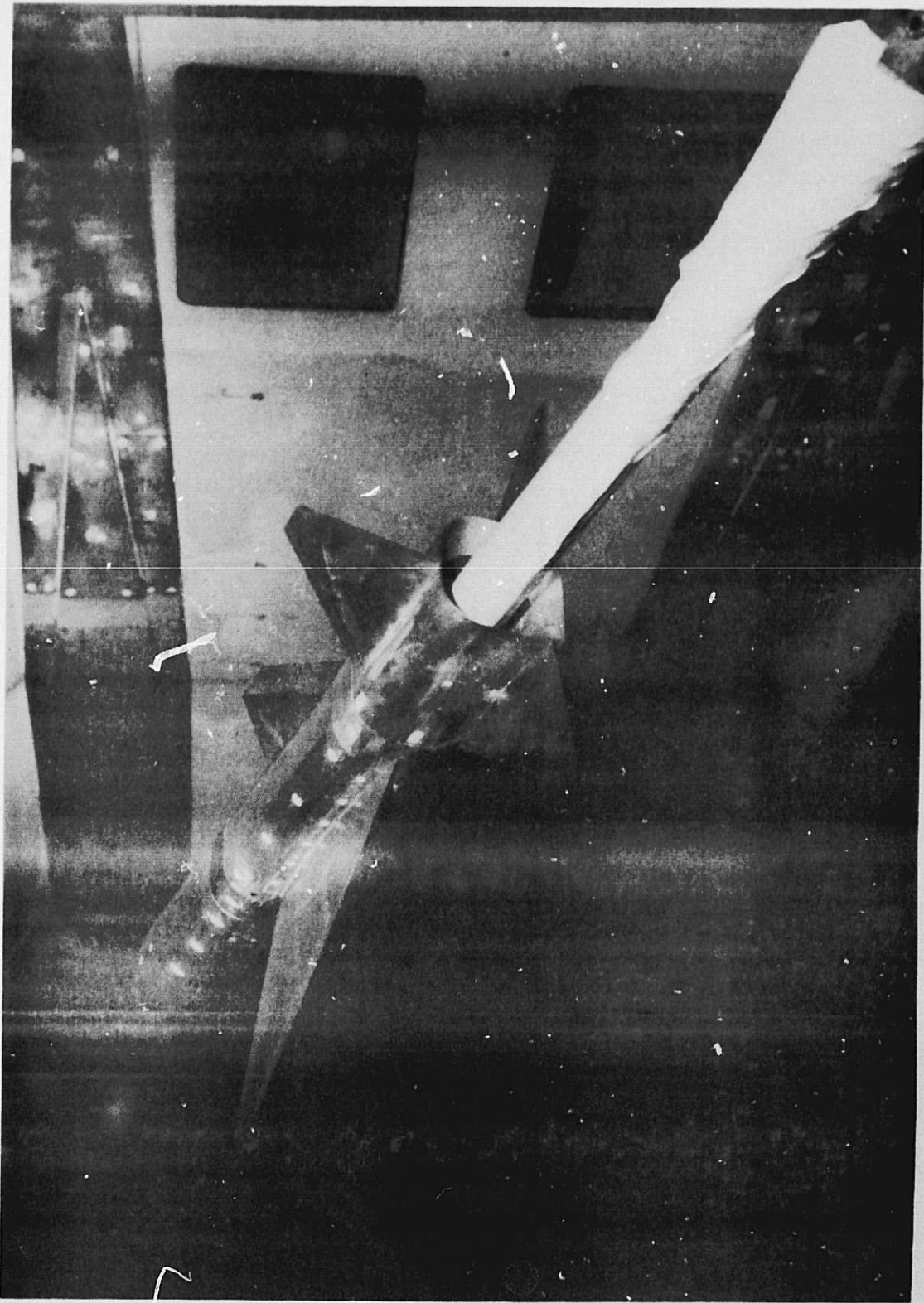
Figure 3.- Swept-forward wing model mounted for the forced-oscillation roll tests in Langley high-speed 7-by 10-foot tunnel.

Fixed balance support

Torque bridge location

Model attachment surface

Heater bands

CENTIMETERS
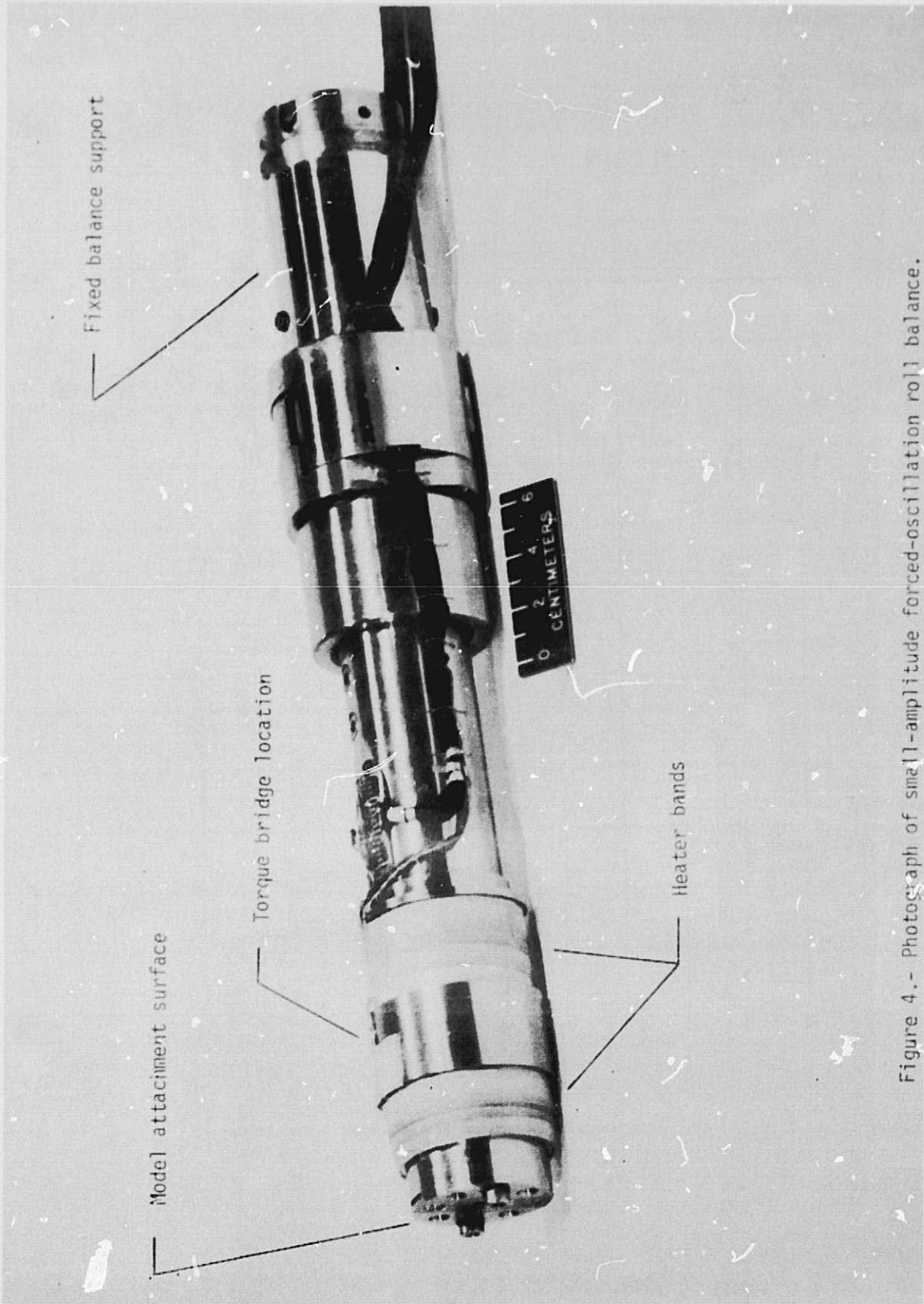
Figure 4.- Photograph of small-amplitude forced-oscillation roll balance.
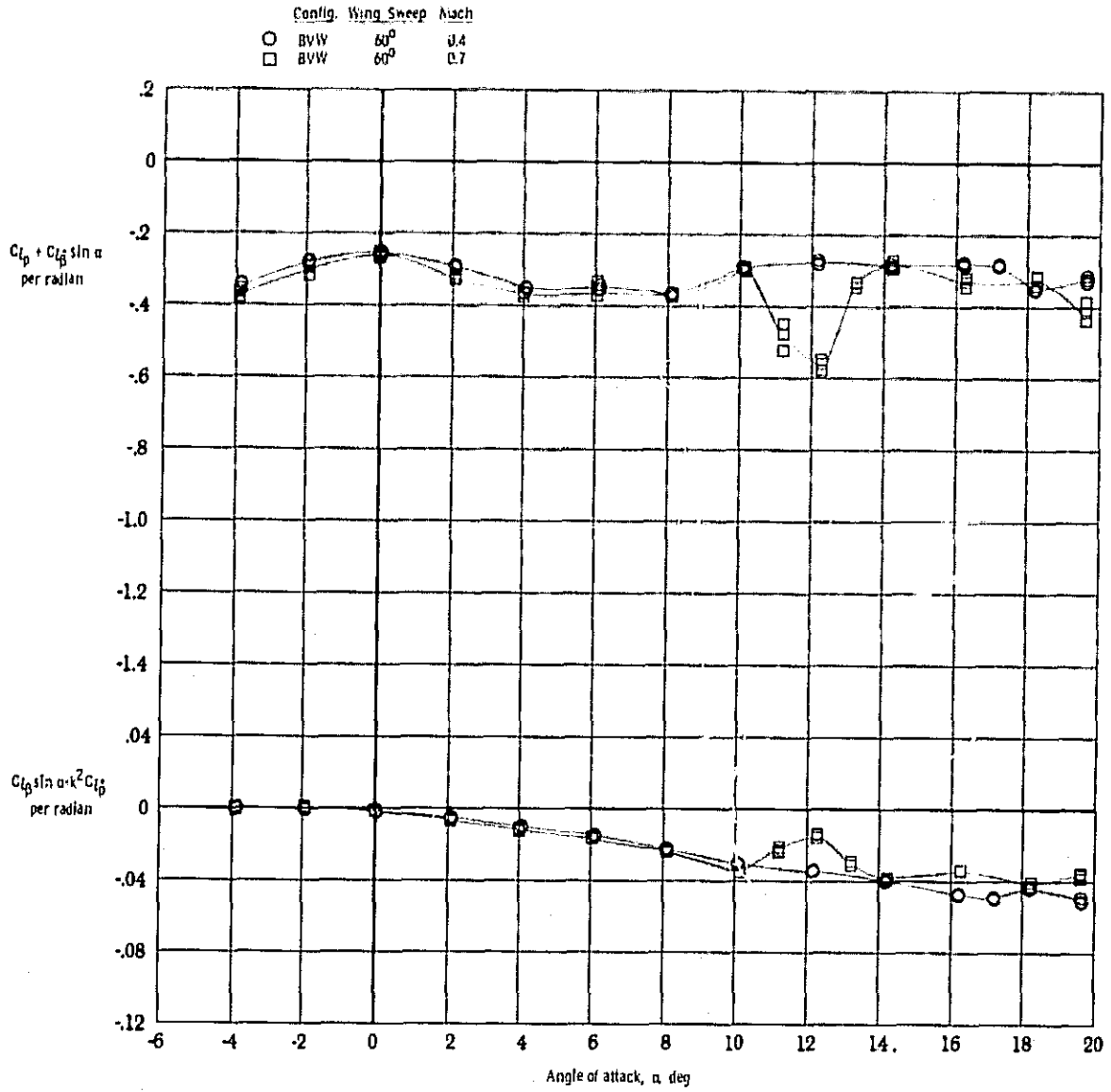
(a) Damping in roll parameter and rolling moment due to roll displacement parameter.

Figure 5.- Effect of Mach number on the 60^0 swept-back wing configuration.
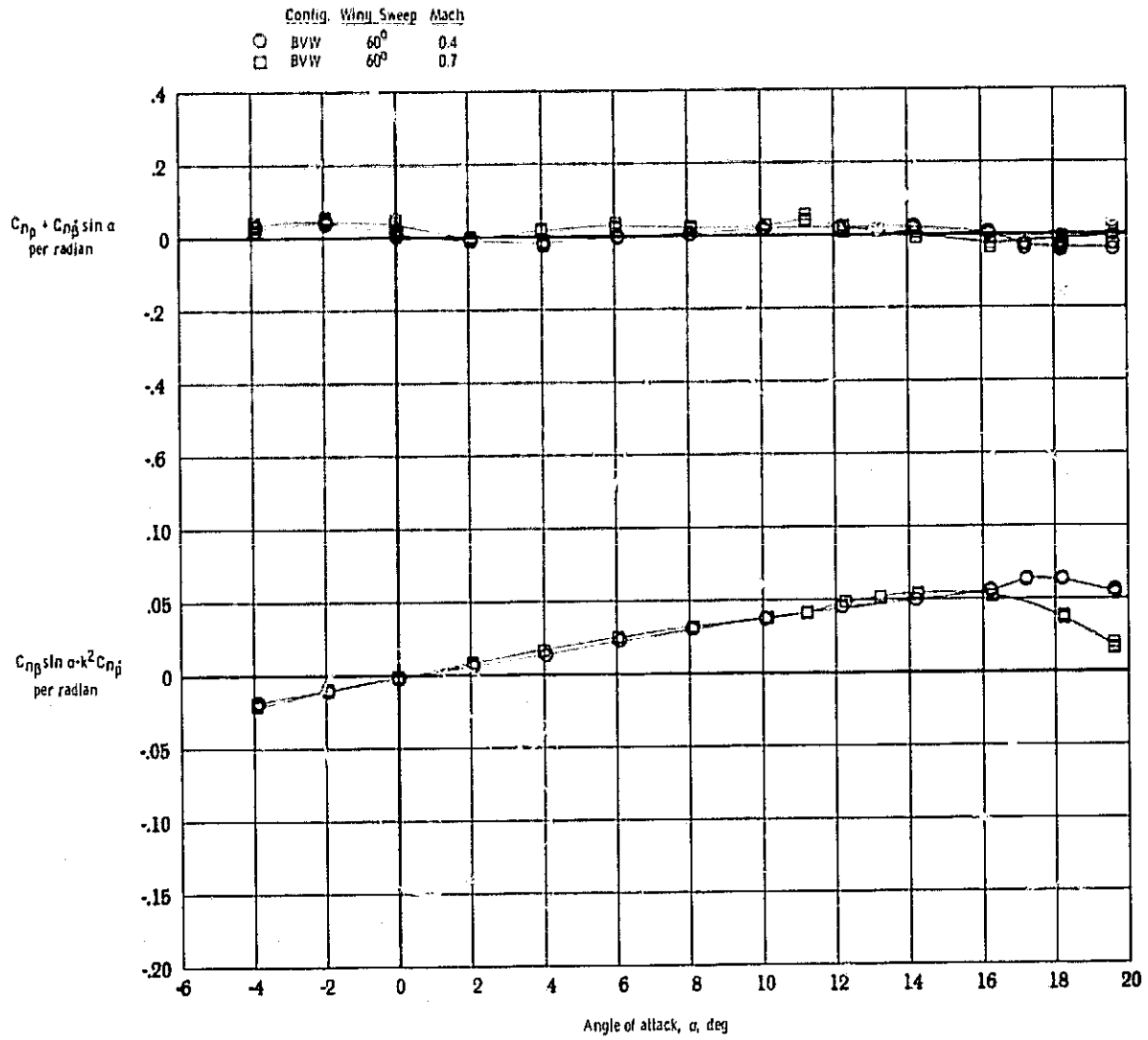
$C_{n_p} + C_{n_\dot\beta} \sin \alpha$
per radian

$C_{n_\beta} \sin \alpha - k^2 C_{n_\dot\rho}$
per radian

Angle of attack, α, deg

(b) Yawing moment due to roll rate parameter and yawing moment due to roll displacement parameter.

Figure 5.- Concluded.
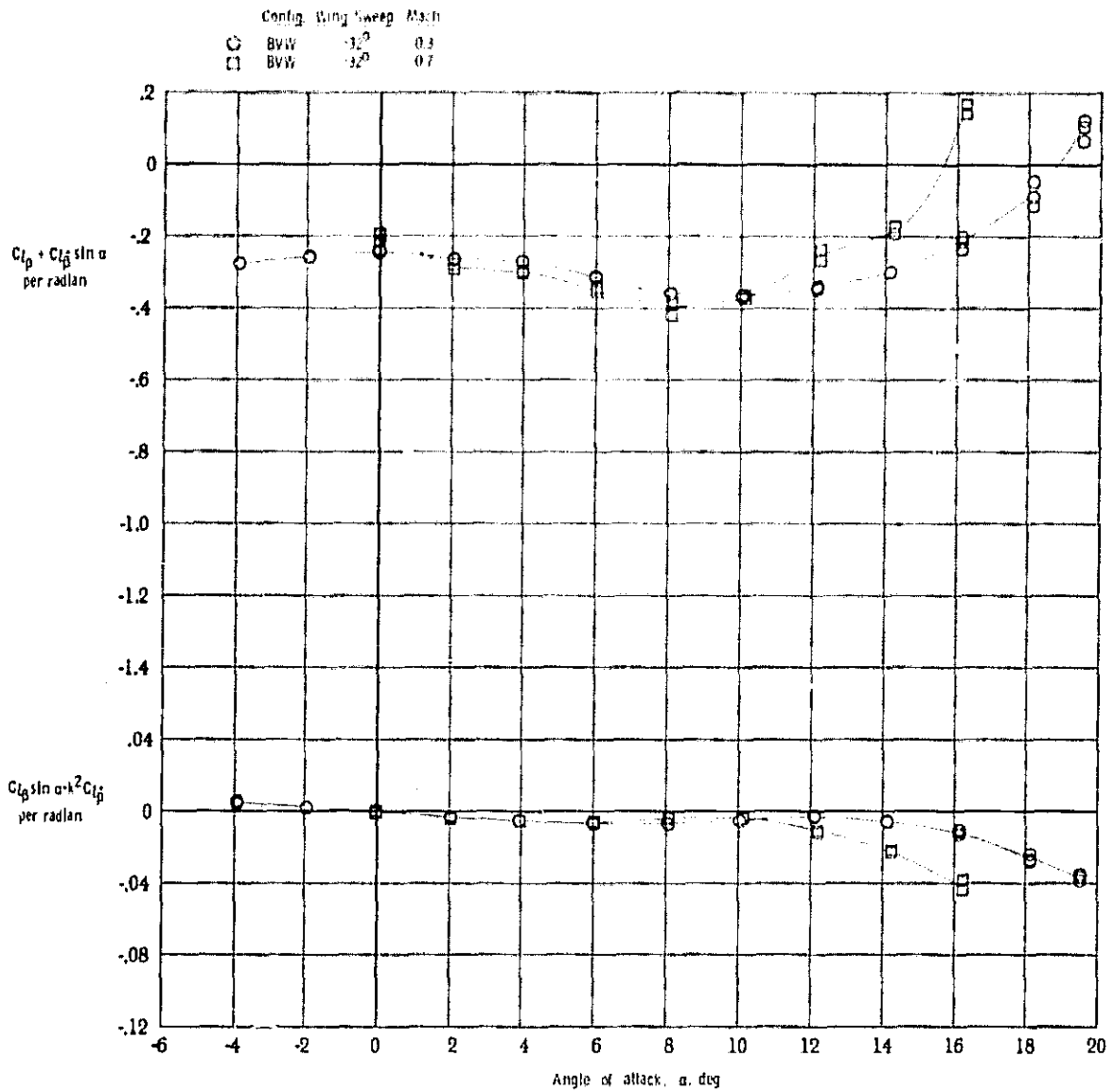
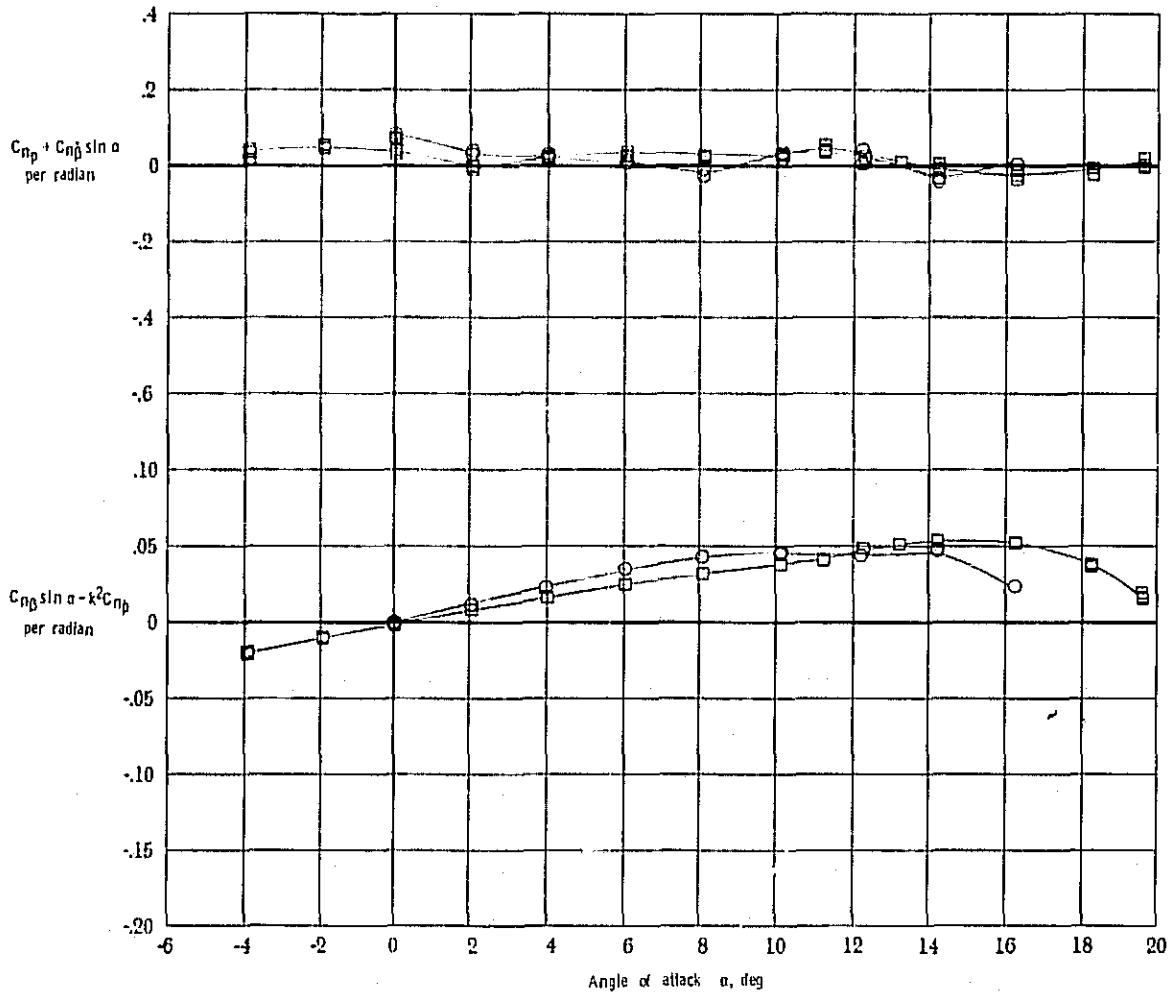(a) Damping in roll parameter and rolling moment due to roll displacement parameter.

Figure 6.- Effect of Mach number on the 32° swept-forward wing configuration.
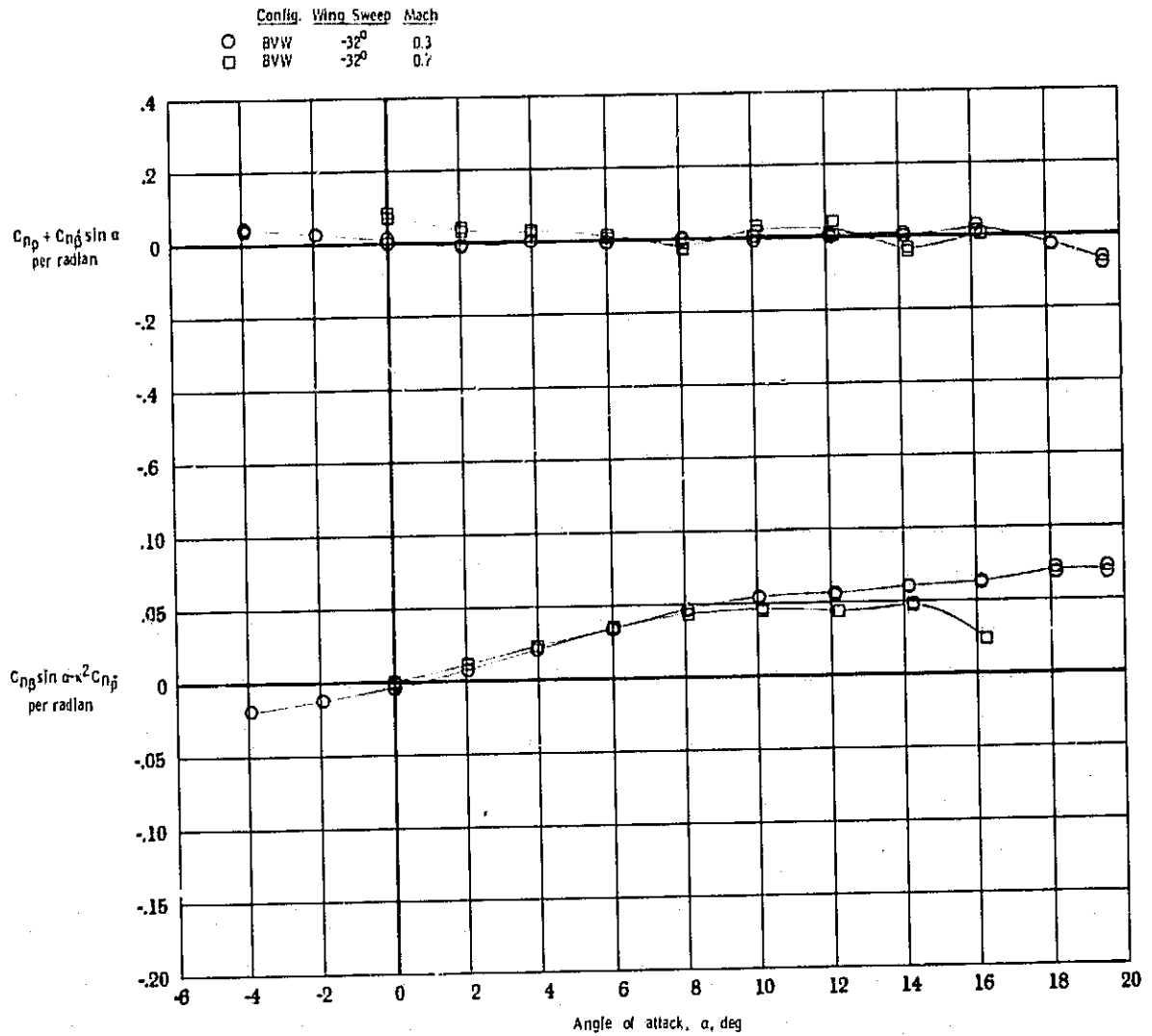
(b) Yawing moment due to roll rate parameter and yawing moment due to roll displacement parameter.

Figure 6.- Concluded.
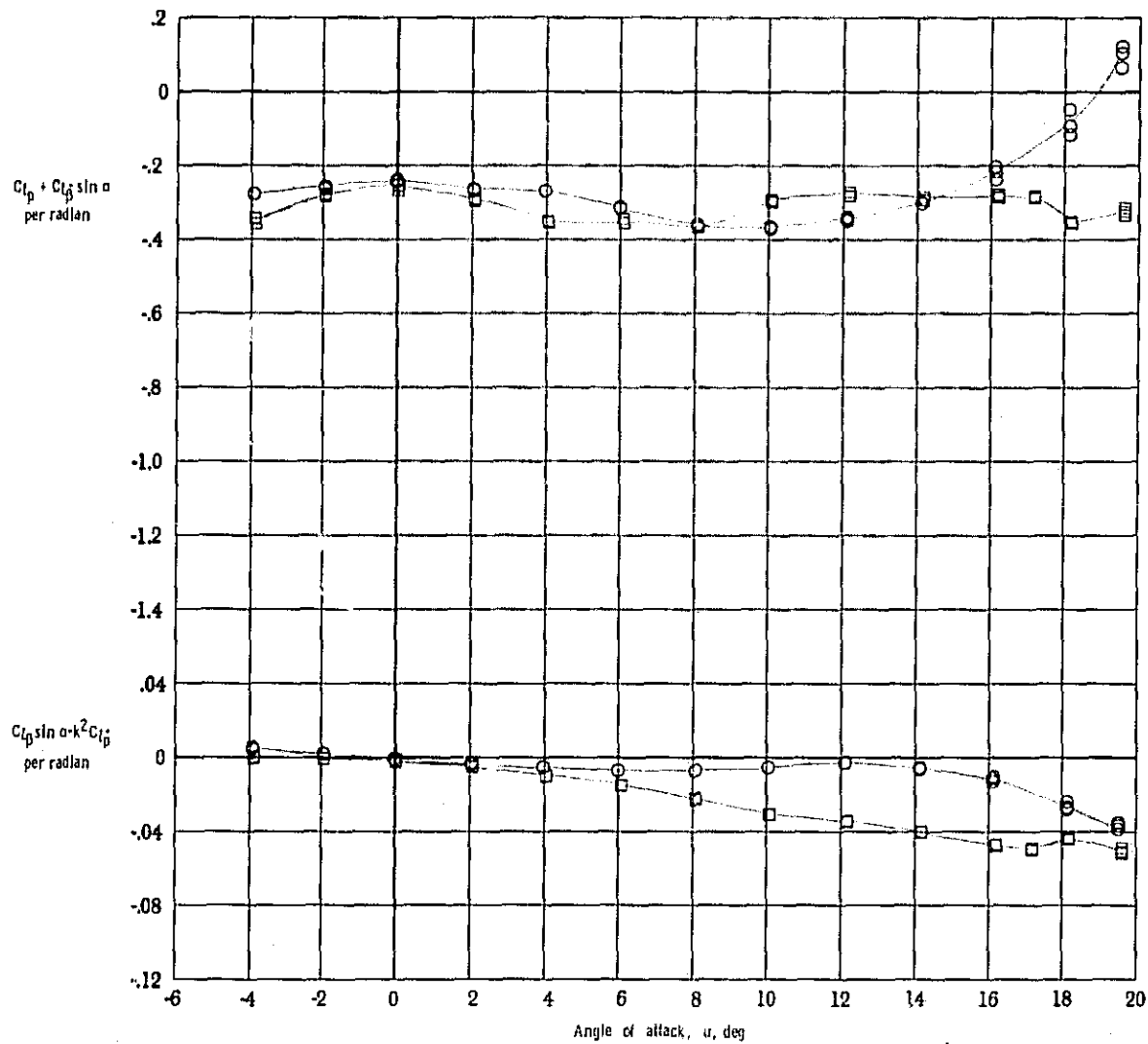
(a) Damping in roll parameter and rolling moment due to roll displacement parameter.

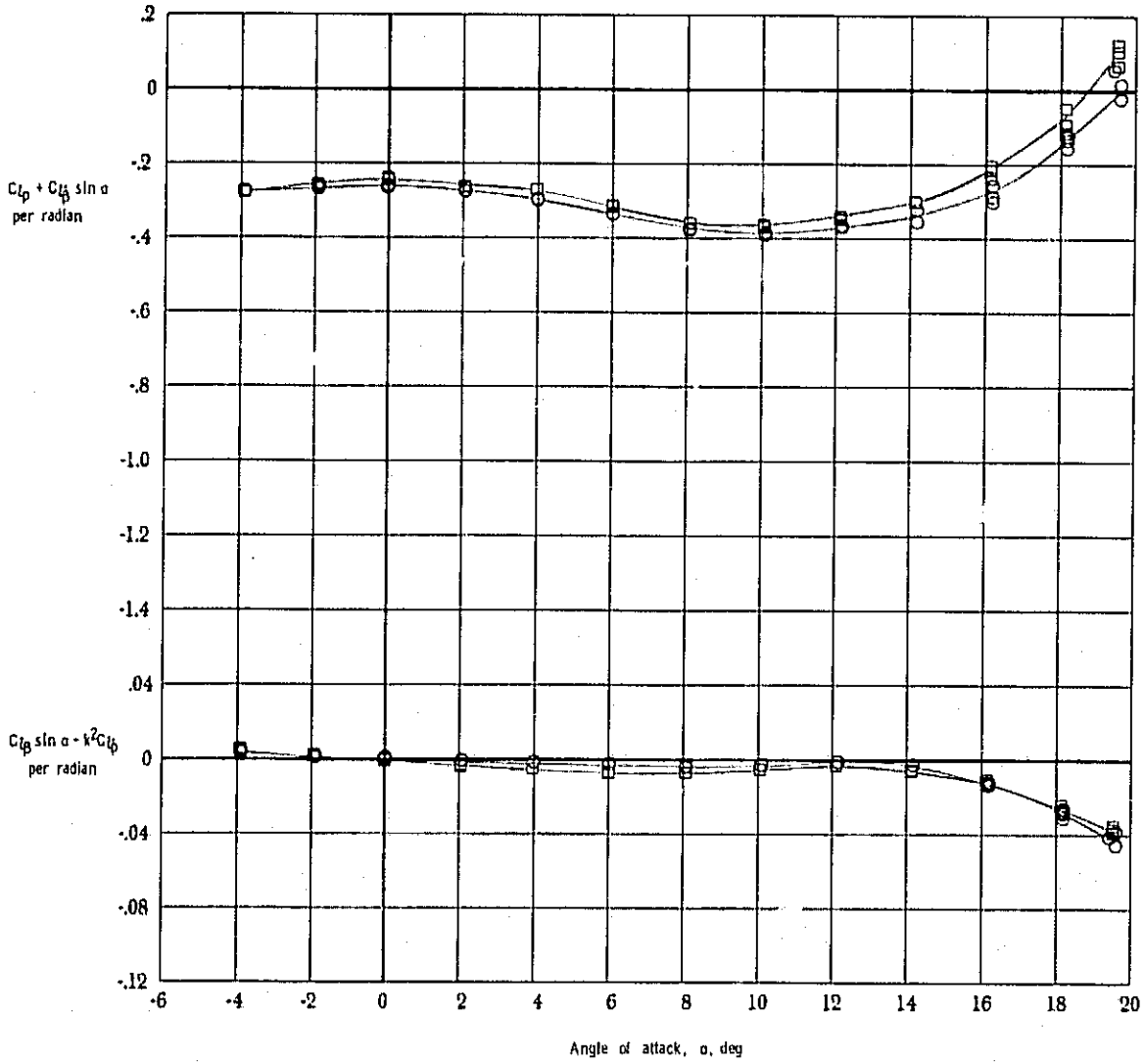Figure 7.- Effect of wing orientation on the body-vertical tail-wing configuration. M = 0.3 and 0.4.
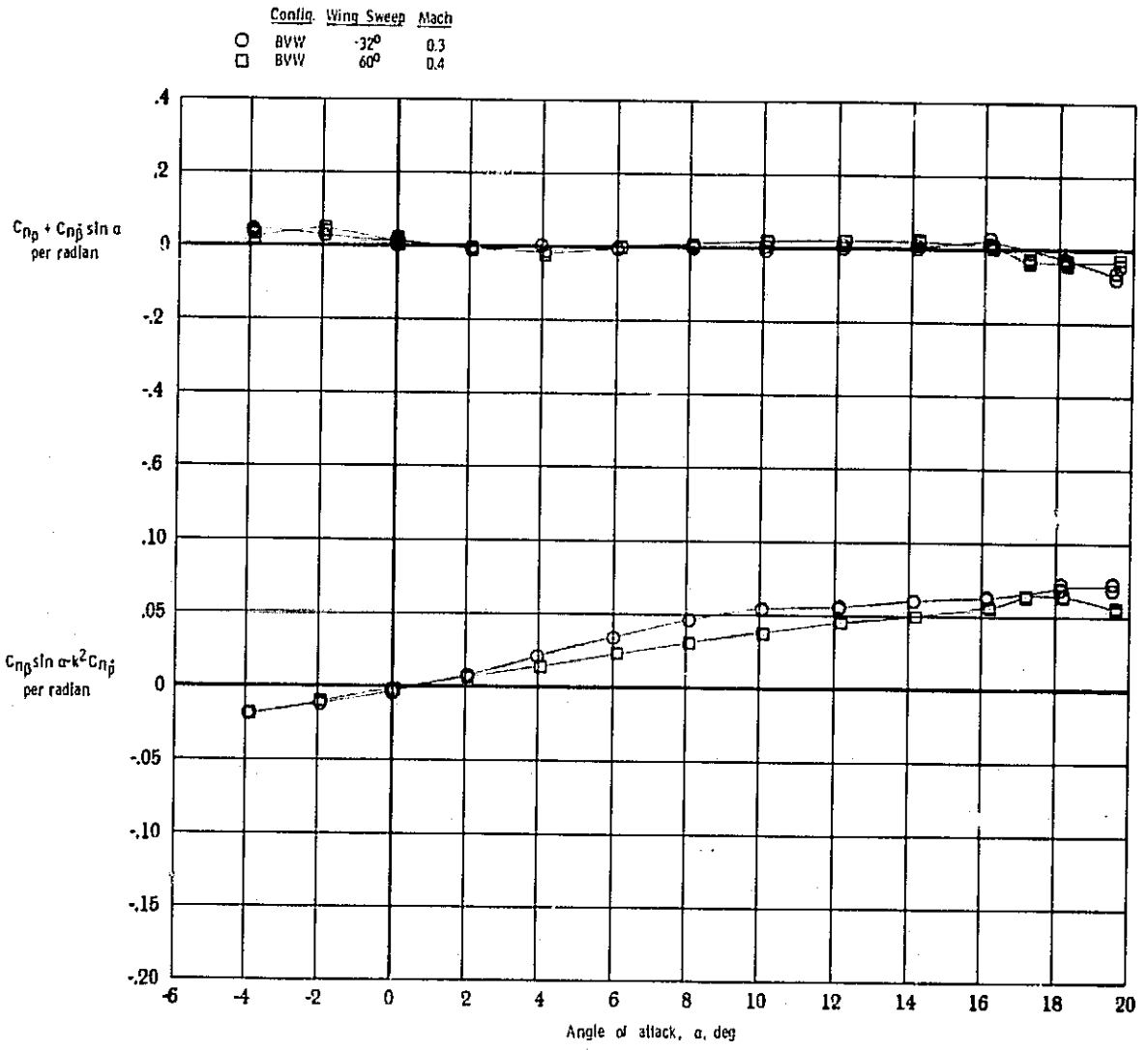
(b) Yawing moment due to roll rate parameter and yawing moment due to roll displacement parameter.

Figure 7.- Concluded.
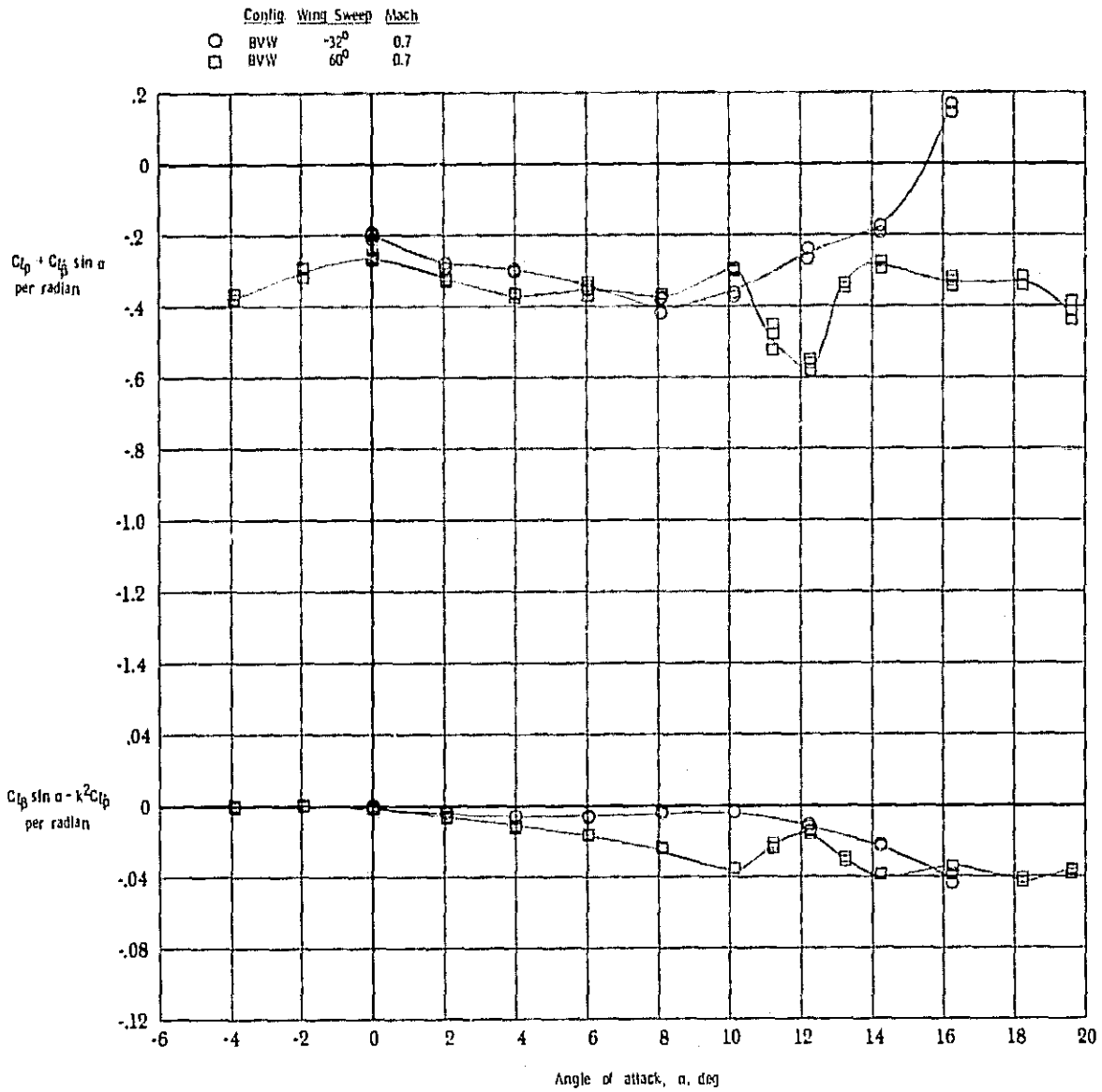
(a) Damping in roll parameter and rolling moment due to roll displacement parameter.

Figure 8.- Effect of wing orientation on the body-vertical tail-wing configuration. M = 0.7.

(b) Yawing moment due to roll rate parameter and yawing moment due to roll displacement parameter.

Figure 8.- Concluded.

(a) Damping in roll parameter and rolling moment due to roll displacement parameter.
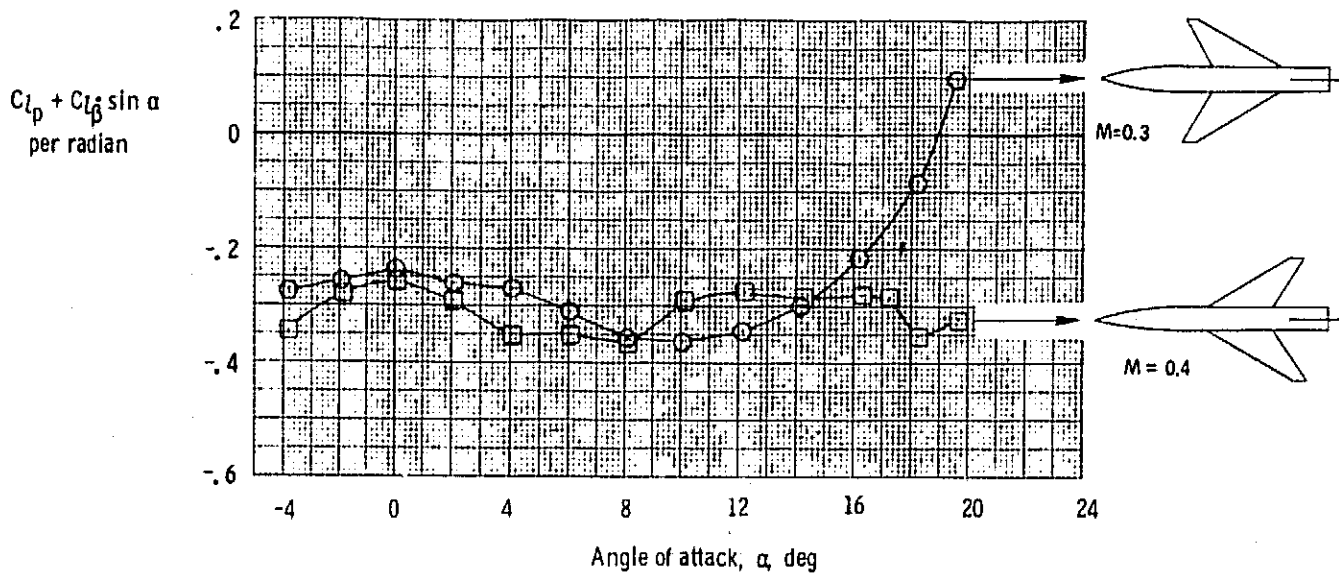
Figure 9.- Effect of horizontal tail on the 32^0 swept-forward wing configuration. $M = 0.3$.
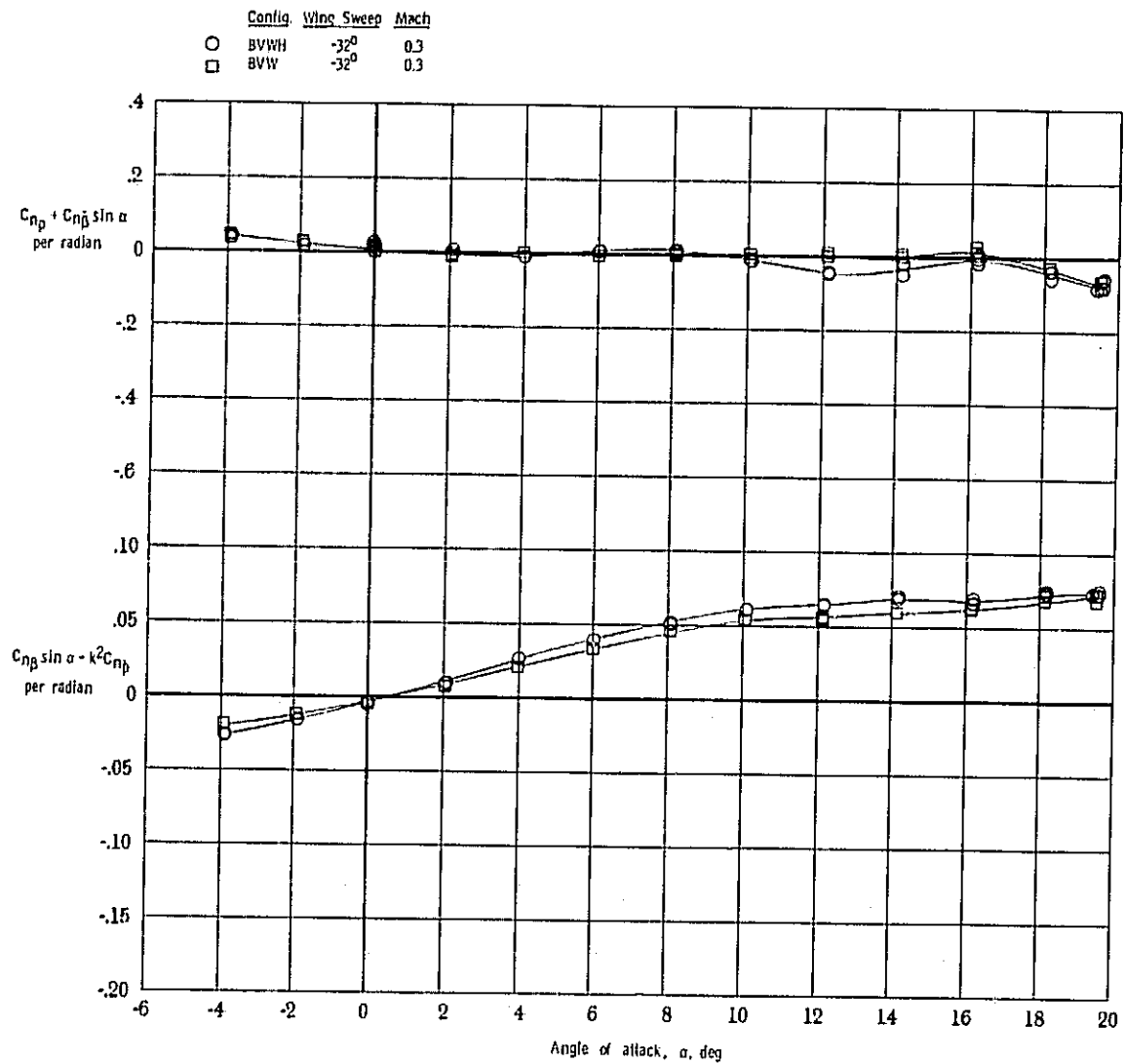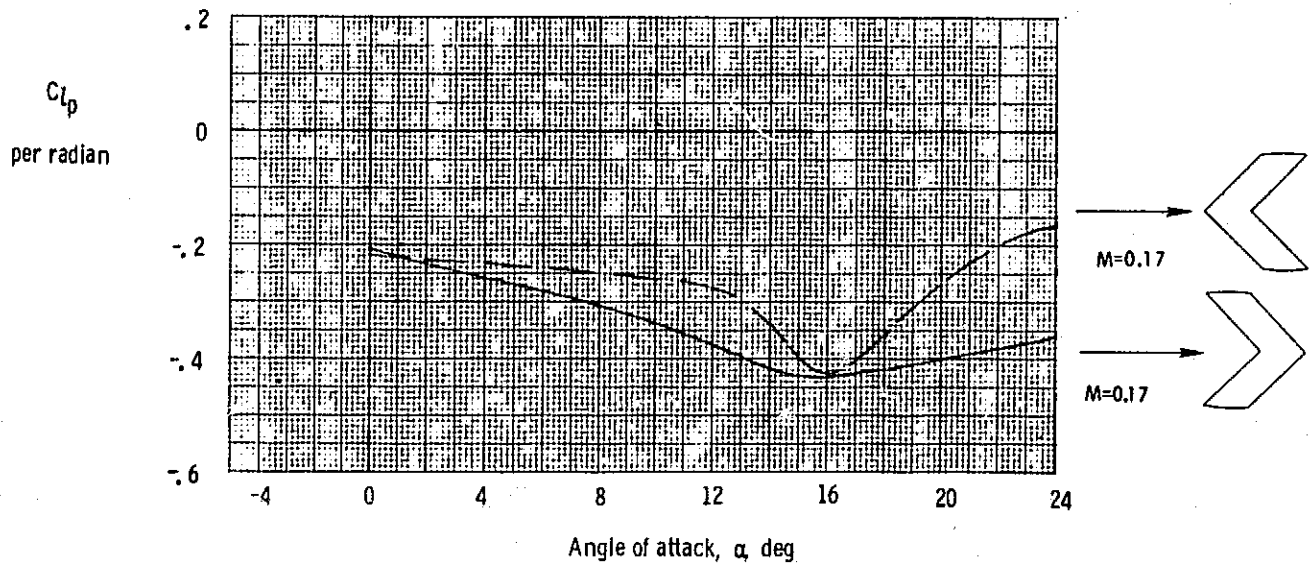
(b) Yawing moment due to roll rate parameter and yawing moment due to roll displacement parameter.

Figure 9. - Concluded.

(a) Circular arc wing section. Configuration BVW, wing sweep = -32° and 60°, aspect ratio = 2.56, taper ratio = 0.19.

(b) NACA 0012 wing section. Configuration W, wing sweep = ±45°, aspect ratio = 2.61, taper ratio ratio = 1.00. (Reference 6)

Figure 10.- Comparison of present sharp leading-edge results with round leading-edge results of reference 6.

1. Report No. NASA TM 78677	2. Government Accession No.	3. Recipient's Catalog No.
4. Title and Subtitle SUBSONIC ROLL DAMPING OF A MODEL WITH SWEPT-BACK AND SWEPT-FORWARD WINGS		5. Report Date March 1978
		6. Performing Organization Code 3850
7. Author(s) Richmond P. Boyden		8. Performing Organization Report No.
		10. Work Unit No.
9. Performing Organization Name and Address NASA Langley Research Center Hampton, Virginia 23665		11. Contract or Grant No.
		13. Type of Report and Period Covered Technical Memorandum
12. Sponsoring Agency Name and Address National Aeronautics and Space Administration Washington, DC 20546		14. Sponsoring Agency Code

15. Supplementary Notes

16. Abstract

The aerodynamic roll damping and the yawing moment due to roll rate characteristics were investigated at subsonic speeds for a model with either swept-back or swept-forward wings. The tests were made in the Langley high-speed 7- by 10-foot tunnel for Mach numbers between 0.3 and 0.7. The configuration with a $60°$ swept-back wing had positive damping in roll up to the maximum test angle of attack of almost $20°$. The $32°$ swept-forward wing configuration had positive damping in roll at the lower angles of attack, but there was a decrease in damping and negative damping in roll was measured at the highest angles of attack.

17. Key Words (Suggested by Author(s)) Swept-Forward Wings Roll Damping Dynamic Stability	18. Distribution Statement Unclassified – Unlimited Star Category – 02

19. Security Classif. (of this report) Unclassified	20. Security Classif. (of this page) Unclassified	21. No. of Pages 34	22. Price* $4.50